

Light Scattering from Random Coils Dispersed in Solutions of Rodlike Polymers

T. Jamil, P. S. Russo,* I. Negulescu, and W. H. Daly

Department of Chemistry and Macromolecular Studies Group, Louisiana State University, Baton Rouge, Louisiana 70803

D. W. Schaefer and G. Beaucage

Division 1703, Sandia National Laboratories, Albuquerque, New Mexico 87185

Received August 17, 1993; Revised Manuscript Received October 8, 1993*

ABSTRACT: The thermodynamics and mobility of a random-coil polymer were studied by light scattering in toluene solutions containing a rodlike polymer. The random-coil polymer was polystyrene (PS). The rodlike polymer was helical poly(γ -stearyl α ,L-glutamate), or PSLG, which aggregates end-to-end in toluene to produce long filaments. As PSLG is almost isorefractive with toluene, the scattering of PS can be measured in PSLG/toluene mixtures with almost no interference from PSLG. The apparent second virial coefficient of the PS component decreases rapidly with addition of the "invisible" rodlike polymer component, while the PS radius of gyration does not. A θ condition is reached at slightly more than 1% added PSLG. Although PSLG and PS probably have a disfavorable interaction parameter, enthalpic interactions are of secondary importance. This point was underscored by experiments involving the addition of 5% dodecane to binary PS/toluene solutions; the small, aliphatic solvent had virtually no effect. The reduction of the virial coefficient, but not the size, of the random-coil polymer in the presence of PSLG is due to the occupation of connected (and linearly correlated) space. Parallel effects were observed in the mutual diffusion coefficient of the coil component, which increased with PS concentration at low rod content but did the opposite when enough PSLG was added. Extrapolated to zero PS content, the mutual diffusion coefficient is expected to approach closely the self-diffusion of trace quantities of PS in the PSLG/toluene solution. So obtained, the self-diffusion coefficient decreased with added rodlike PSLG, but not as fast as the viscosity increased; thus, the Stokes-Einstein relationship was not obeyed by PS probes in PSLG/toluene solutions. Scaling arguments are presented for the dependence of the size of a random coil in the presence of rods and for the crossover from Stokes-Einstein diffusion of the coil to a reptative type of motion. The available data are not well suited to test these relationships, due to limitations in the matrix concentration imposed by polymer incompatibility.

Introduction

Diffusion of macromolecules and colloidal particles in various complex solutions continues to attract much attention. Experimental systems typically contain a probe whose translational diffusion is to be measured, a matrix that may restrain the probe, and a solvent. We use the notation probe/matrix/solvent to distinguish among systems. Sphere/random coil/solvent systems¹⁻⁵ are ostensibly the simplest. Nevertheless, serious questions still remain, including the degree of adherence to continuum expressions like the Stokes-Einstein relationship between diffusion and viscosity. Random coil/random coil/solvent and random star/random coil/solvent systems have been extensively studied.⁷⁻²² An objective of these studies is to determine the applicability of reptation theory to polymer solutions.²³ In a few cases, the matrix has been a gel²⁴⁻²⁶ or another permanent, porous structure.^{27,28} There have been a few sphere/rod/solvent studies,²⁹⁻³⁴ but little is known of random coil/rod/solvent or rod/random coil/solvent systems.

This paper concerns the behavior of a random-coil probe in a mixture comprised of nonionic rodlike polymer and organic solvent. The limited solubility of rods, their tendency to form mesophases, and their poor miscibility with random coils³⁵ pose serious experimental challenges. The measuring technique can itself impose additional limitations—for example, optical tracer measurements require attachment of an appropriate dye, while dynamic light scattering is simplest when the solvent is isorefractive

with the polymeric matrix. Nevertheless, mixtures of rods and coils in a solvent are important, for they occur naturally and are also the precursors to rigid rod/random coil molecular composites.³⁶ In the present study, dynamic and static scattering of a random coil (polystyrene, PS) is measured in the presence of semiflexible poly(γ -stearyl α ,L-glutamate), or PSLG, codissolved in toluene. PSLG is a linear homopolymer³⁷⁻⁴⁰ related to the commonly studied poly(γ -benzyl α ,L-glutamate) (PBLG). Although PSLG's persistence length is not known, the Mark-Houwink exponent of 1.29 ± 0.09 measured^{37,39} in tetrahydrofuran (THF) for unfractionated samples suggests a polymer of considerable rigidity. The aliphatic side chain of PSLG is longer than PBLG's stubby aromatic side chain, imparting even greater solubility and useful optical properties. In particular, PSLG is virtually invisible in toluene, so practically all of the scattering in the PS/PSLG/toluene system arises from the PS.

The principal variables in this study are the concentrations of random-coil and rodlike components and the scattering vector. The PS concentrations were kept in the dilute solution regime, whereas the PSLG matrix concentration was bounded by the requirement that both polymers remain in a homogeneous solution. Specifically, the concentration ranges in the present study are 0.0005–0.004 g/mL for PS (i.e., $0.0005 < c_{PS} < 0.004$) and 0.001–0.015 g/mL for PSLG solutions ($0.001 < c_{PSLG} < 0.015$). This corresponds to $0.03 < x < 0.8$ for the ternary solutions, where x is $c_{probe}/c_{total} = c_{PS}/(c_{PS} + c_{PSLG})$. If c^* represents an overlap concentration (defined for convenience as $[\eta]^{-1}$, where $[\eta]$ is the intrinsic viscosity), then $0.14 < c/c^*_{PS} < 1.13$. It is more difficult to define c^*_{PSLG} in terms of its inverse intrinsic viscosity, for reasons that will become apparent.

* To whom correspondence should be addressed.

Abstract published in *Advance ACS Abstracts*, November 15, 1993.

Theoretical Background

No theory directly treats the static and dynamic light scattering from a random coil in a rod-bearing solution. We rely upon more general developments for ternary probe/matrix/solvent systems,^{41–50} restricting the discussion primarily to theories developed for polymeric probes in isorefractive matrix/solvent mixtures.^{45–50} Using the random-phase approximation, Benmouna and co-workers^{45–47} showed that, in a ternary system where only one polymer is visible, the normalized electric field autocorrelation function $g^{(1)}(q, \tau)$ can be written as a sum of two exponentials:

$$g^{(1)}(q, \tau) = A_I \exp(-\Gamma_I \tau) + A_C \exp(-\Gamma_C \tau) \quad (1)$$

The decay rates, Γ_I and Γ_C , depend on the thermodynamic and hydrodynamic properties of the system entirely differently. The slower interdiffusion mode, with decay rate Γ_I , corresponds to the relative concentration fluctuations of each polymer species with respect to the other and depends only on the interaction between the two types of monomers. The faster mode, with decay rate Γ_C , is called the cooperative mode and corresponds to fluctuations of the total polymer concentration.

It is emphasized that the existence of easily identifiable interdiffusion and cooperative modes in ternary polymer solutions is hardly guaranteed. An experimental requirement is that there be adequate amplitude for each mode, which is true when x exceeds ~ 0.1 .¹⁴ There must also be a significant—meaning at least a factor of 2—separation in the decay rates. Even if the modes can be separated experimentally, Akcasu et al. have set forth stringent requirements upon the similarity of the two polymers before the two modes should be interpreted as interdiffusion and cooperative diffusion.^{49,50} Suffice it to say, the present experiments with a random-coil probe and rigid-rod matrix fail to meet these requirements. But when the visible probe polymer is present in its dilute concentration regime and when the matrix is properly index matched, the slower mode clearly dominates. Under such conditions, and at sufficiently low values of the scattering vector magnitude, q , the measured average decay rate, $\bar{\Gamma}$, is proportional to the mutual diffusion coefficient D_m of the strongly scattering component through the complex “solvent” comprised of a matrix polymer and small molecule. In the limit of zero concentration of the strong scatterer, D_m approaches the probe self-diffusion coefficient D_s . Thus, D_s of the visible probe can be measured by extrapolating $\bar{\Gamma}/q^2$ first to zero scattering vector and then to zero x at constant c_{matrix} .

Experimental Section

Poly(γ -stearyl α ,L-glutamate) was synthesized from monomer to make a pure homopolymer, as described previously.⁴⁰ A tertiary amine initiator was used, so that no initiator is attached at the beginning of the chain. Static light scattering in THF gave a molecular weight of 32 000. From the monomer repeat mass, 382 g/mol, and using the projection length of a monomer repeat along an α -helix, 1.5 Å, we compute a contour length $L = 126$ Å. The diameter of PSLG is about 37 Å, so the axial ratio is $L/d = 3.4$. Polystyrene of advertised molecular weight 1.26×10^6 was purchased from Toyo Soda Manufacturing Co. (Type F-128). Glassware (at critical stages) and scattering cells (always) were tested for cleanliness by using the light scattering spectrometer's 100 \times viewing port to observe the laser beam traverse the vessel of interest or, for large containers, a cleaned vial containing the rinse from that vessel. Toluene of spectroscopic grade was purchased from Aldrich, filtered through selected, prefabricated 0.02- μm Anotop filters into precleaned and tested cells, and then centrifuged at ca. 3500g for several days until completely free of dust. PSLG used for the ternary samples was dedusted by

filtering THF solutions through selected 0.2- μm prefabricated Anotop filters into a cleaned and tested vial, followed by vacuum drying at 50 °C for 1 week. Stock solutions were prepared by adding filtered/centrifuged toluene to known amounts of PSLG and PS. Stock solutions of PS were filtered through selected, prefabricated 0.2- μm Anotop filters. Ternary solutions were prepared directly in the cleaned and tested scattering cells (simple Pyrex 13 \times 75 mm test tubes) by mixing known volumes of centrifuged solutions of PSLG, PS, and solvent. The cells were sealed with poly(tetrafluoroethylene)-faced screwtop lids. All measurements were made at 25.0 ± 0.1 °C.

The light scattering spectrometer is similar to the one described elsewhere.^{31,51} A Lexel Model 95-2 Ar⁺ ion laser producing up to 1.4 W, vertically polarized, at $\lambda_0 = 5145$ Å was operated in constant current mode for dynamic measurements and in constant intensity mode for static measurements. All polarization components of the scattered light were detected. Almost all of the correlation functions were measured using an EMI-9863A/100 photomultiplier tube selected for low correlated afterpulsing and low dark counts, a Pacific Precision Model 126 photometer, and a 272-channel Langley-Ford Model 1096 correlator, operated in linear mode. The channel (sampling) time of the correlator was set to ensure complete decay of the measured correlation function; typically, 63% of the decay occurred within the first 32 channels. The correlation functions were analyzed by the method of cumulants,⁵² with exceptions as noted. In order to determine the scattered spectrum over a very wide range, a few measurements were made using an ALV-5000 digital autocorrelator, connected to a separate measurement system.

Static measurements were made on the same samples, in the same cells, and with the same instrument, except for the substitution of a Hamamatsu R928P photomultiplier tube. Compared to the dynamic measurements, the optical coherence was decreased to improve the signal-to-noise ratio (by increasing the number of random events to nearly match the number of photocounts, as compared to the much smaller ratio of acquisition time to correlation time⁵³). Five repeat runs, each of several seconds duration, were used to obtain the intensity and corresponding uncertainty at each concentration and angle. The scattering volume at each angle θ obeyed a simple $(\sin(\theta))^{-1}$ relationship, typically, to 1% over the measured angular range (30–130°); additional volume “corrections” were not applied. Uncertainties in the measured parameters are routinely derived from standard propagation of error formulas; however, systematic error is usually the more serious concern, and we estimate that the measurements are only accurate to within $\pm 10\%$. Toluene was used as a Rayleigh standard ($\mathcal{R}_{\theta=90^\circ} = 32.08 \times 10^{-6} \text{ cm}^{-1}$ for detection of all polarization components scattered from a vertically polarized incident beam^{54,55}).

The macroscopic viscosities of PSLG/toluene solutions were measured on a Brookfield LVTDCP cone & plate viscometer. An extrapolation to zero-shear rate was made, although shear thinning was very minor in the usable shear rate range (75–450 s⁻¹). The intrinsic viscosity of PSLG in toluene, tetrahydrofuran, and toluene/methyl ethyl ketone mixtures (95/5% by volume) was measured in an Ubbelohde viscometer at 25.0 ± 0.05 °C. The flow time for pure toluene was 183 s; kinetic energy corrections were not applied.

Neutron scattering experiments were performed at the Oak Ridge National Laboratories High Flux Isotope Reactor using a wavelength of 10 Å. A 1.5% PSLG solution in toluene- d_8 was investigated in a 1-mm-path-length quartz cell. The data were corrected for background, detector sensitivity, and empty cell scattering and converted to absolute intensity. Incoherent scattering from toluene- d_8 was insignificant, as can be seen by the absence of a flat incoherent background in the data at the highest values of the scattering vector.

Data Analysis

Static light scattering intensity data were analyzed according to an expression adapted from dilute binary solutions:⁵⁶

$$RTKc_{\text{PS}}/\mathcal{R}_\theta = (\partial\pi/\partial c_{\text{PS}})_{T,p}(1 + q^2\xi^2 + \dots) \quad (2)$$

On the left-hand side, R is the gas constant, T is the

absolute temperature, and K is an optical constant: $K = 4\pi^2 n^2 (dn/dc)^2 \lambda_0^{-4} N^{-1}$, where n is the solution refractive index, dn/dc is the probe specific refractive index increment, λ_0 is the wavelength in vacuo, and N is Avogadro's number. The Rayleigh factor, \mathcal{R}_θ , is proportional to the measured excess intensity (above the PSLG/toluene complex solvent) scattered through angle θ . On the right-hand side are the parameters of interest. $(\partial\pi/\partial c_{PS})_{T,p}$ is the osmotic modulus, $q = (4\pi n/\lambda_0)\sin(\theta/2)$ is the magnitude of the scattering vector, and ξ is the scattering correlation length, equal to $R_{g,PS}/3^{1/2}$ in the limit $c_{PS} = 0$, where $R_{g,PS}$ is the probe radius of gyration. As the polystyrene under consideration is not very large, $(\partial\pi/\partial c_{PS})_{T,p}$ could be obtained satisfactorily from a linear extrapolation to $q^2 = 0$. The square root of the slope/intercept ratio gives ξ at a particular concentration. Probe radius of gyration can be determined by extrapolating ξ to $c_{PS} = 0$. Apparent R_g values can also be obtained from Guinier plots ($\ln \mathcal{R}_\theta$ vs q^2 ; the slope is $R_{g,app}^2/3$). This method has the advantage that the apparent size is insensitive to errors in the intercept. $R_{g,PS}$ values in the present study come from extrapolating $R_{g,app}$ from Guinier plots to $c_{PS} = 0$.

In binary solutions of random coils in good solvents, plots of $(\partial\pi/\partial c)_{T,p}$ vs c often exhibit significant curvature. Linear Zimm plot analysis⁵⁷ of such curved data can produce serious errors.⁵⁸ Kent et al.¹⁹ have pointed out the special danger that curvature poses for studies in ternary solutions—specifically, that the error associated with a linear Zimm-type analysis changes as the matrix polymer is added, leading to false trends in probe molecular weight, size, and virial coefficient. To circumvent these problems, the (weight-average) molecular weight, M_{PS} , and osmotic second virial coefficient, $A_{2,PS}$, of the probe were obtained from quadratic fits to $(\partial\pi/\partial c_{PS})_{T,p}$ vs c_{PS} . The differences between linear and quadratic analyses were significant in pure toluene and at low PSLG content but essentially vanished under binary θ conditions (cyclohexane at 34.7 °C) and at higher PSLG contents.

In the homodyne mode, and assuming Gaussian fluctuations, $g^{(1)}(\tau)$ is determined from the intensity autocorrelation function $G^{(2)}(\tau) = B[1 + f_{coh}g^{(1)}(\tau)]^2$ where B is a base line and f_{coh} is an instrument parameter ($0 < f_{coh} < 1$) depending primarily on the number of coherence areas detected, at least for strongly scattering samples. For monodisperse, spherical, and optically isotropic particles, $g^{(1)}(\tau)$ is a single exponential, $g^{(1)}(\tau) = \exp(-\Gamma\tau)$, where $\Gamma = D_m q^2$. Systems that exhibit a distribution of decay times can be characterized by a cumulant expansion⁵²

$$\ln g^{(1)}(\tau) = -\bar{\Gamma}\tau + \mu_2\tau^2/2 - \mu_3\tau^3/6 + \dots \quad (3)$$

Here, $\bar{\Gamma} = -[d \ln g^{(1)}(\tau)/d\tau]_{\tau=0}$ is the first cumulant and μ_2 and μ_3 are the second and third cumulants. A given correlation function was collected as a series of about five short runs. Each was analyzed for consistency of intensity, decay rate from a second-order cumulant fit (using the base line B_t to be discussed shortly), degree of nonexponentiality, channel-to-channel correlation of residual errors, and weighted residual of fit. The excellent consistency among short runs ($\bar{\Gamma}$ from a second-order cumulants analysis typically agreed to within $\pm 2\%$) enabled most of the runs to be summed together. From the summed correlation function, representing typically 300–1000 s of data acquisition, $\bar{\Gamma}$ was determined from third-order cumulants, 3CUMU, analysis using a theoretical base line $B_t = P(P - O)/N$, where P , N , and O are respectively the total number of pulses, sample time intervals, and shift register overflows during the acquisition time, to compute $g^{(1)}(\tau)$. Despite moderately long acquisitions

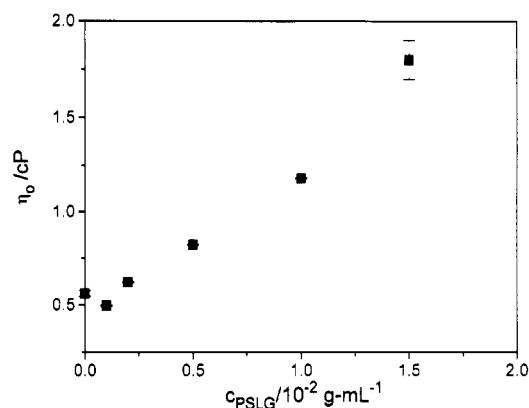


Figure 1. Viscosity of PSLG/toluene solutions.

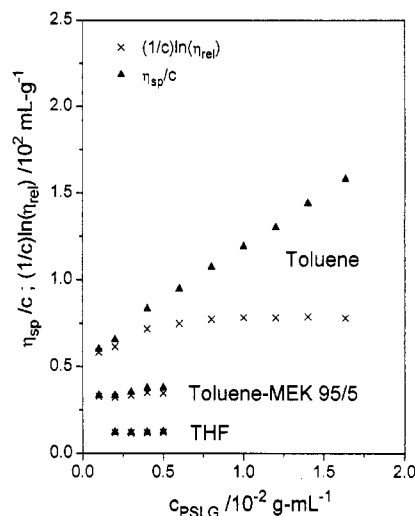


Figure 2. Reduced relative (×) and specific (▲) viscosities in pure toluene, 95% toluene/5% MEK, and THF. End-to-end aggregation in toluene is partly defeated by addition of the hydrogen-bond competitor, MEK.

resulting in B_t of 10^7 – 10^8 , shift register overflows were almost never encountered. Data were weighted according to the standard propagation of errors, based on the uncertainty in $G^{(2)}(\tau)$ being $\sigma_{G^{(2)}(\tau)} = [G^{(2)}(\tau)]^{1/2}$. Channels for which the uncertainty in the normalized, base-line-subtracted correlation function exceeded $1/3$ of the signal were assigned zero weight by the 3CUMU fit. Fits to single exponentials with a floating base line gave decay rates that were virtually identical to the 3CUMU fits, and the fitted base lines B_f were within a few standard base-line uncertainties of B_t .

Results and Discussion

Nature of PSLG in Toluene. The viscosity of PSLG/toluene increases with c_{PSLG} , as shown in Figure 1. The solutions are remarkably viscous for such a stubby rodlike polymer. Moreover, the apparent intrinsic viscosity of PSLG is higher in toluene than in THF, a nonaggregating solvent in which viscosity and light scattering measurements show sensible radius of gyration, virial coefficient, and hydrodynamic behavior for a rodlike polymer.^{37,39} Figure 2 shows specific and relative viscosities (η_{sp} and η_{rel} , respectively) for PSLG/toluene, PSLG/THF, and PSLG/(95 vol % toluene/5 vol % methyl ethyl ketone). Methyl ethyl ketone (MEK) is a hydrogen-bond competitor known to disrupt end-to-end aggregation of PBLG in toluene.⁵⁹ These results suggest that PSLG aggregates end-to-end in toluene. The likely driving force for such aggregation is continued helix propagation. It is not known whether all PSLG's exhibit aggregation; use of primary amine initiators during polymerization often results in

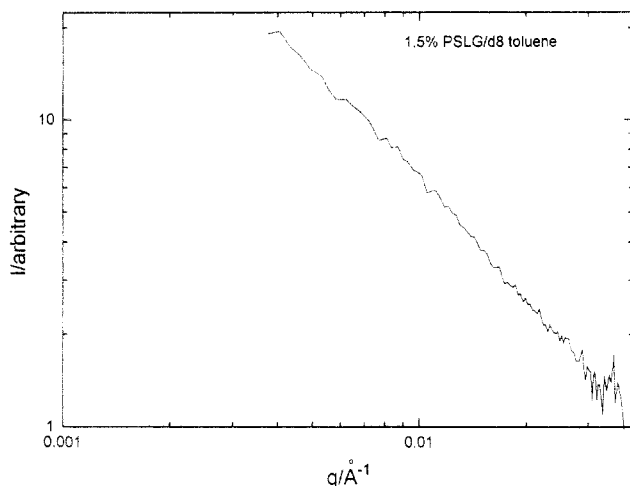


Figure 3. Small-angle neutron scattering by 1.5% PSLG/toluene- d_8 . The absence of a Guinier regime and the power law slope indicate that large, linear aggregates are present.

attachment of the initiator, which may prevent end-to-end associations from occurring. The degree of aggregation in toluene solution depends on the concentration, but a lower limit can be estimated by comparing the apparent intrinsic viscosity to the Mark-Houwink plot determined (on unfractionated samples) for PSLG in THF. We estimate that about five polymers are end-linked to give a total average filament length L_f of about 600 Å. Defining c^* as the inverse of the apparent intrinsic viscosity in toluene (not the only or even the best choice for a rodlike polymer), we obtain $c^* = 0.02$ g/mL, and the range of PSLG concentrations is $0.05 < c/c^* < 0.77$. The product of the filament number density, ν_f , and L_f^3 ranged from about 1 to about 10. This product reflects the crowding in terms of how many aggregated filaments, assuming pentamers, are in a cube of side L_f .

Figure 3 shows the intensity, I , of neutrons scattered from a 1.5% PSLG/toluene- d_8 mixture. The distance scale $2\pi/q$ extends to approximately 1600 Å, adequate to cover the Guinier regime of individual rods ($L = 126$ Å) if they were the predominant scattering species. The absence of a Guinier regime suggests fibrils of large but indeterminate size. The power law exponent (mass fractal dimension⁶⁰) from these data is 1.3 ± 0.05 , indicating an extended structure for the filamentous aggregates. The present data are not quiet enough to obtain the cross-sectional radius of gyration, R_c , from the equation⁶¹ $qI \sim \exp(-q^2R_c^2/2)$. However, a large cross-sectional radius is not indicated. The diameter of a single polymer chain, determined from the virial coefficient in THF^{37,39} is 37 ± 6 Å.

The aggregation problem is compensated by two important characteristics of the PSLG/toluene system: invisibility of the polymer and its ability to remain in solution with PS over an interesting composition range. We attempted to determine the specific refractive index increment dn/dc of PSLG in toluene with a standard Brice-Phoenix divided-cell differential refractometer adapted and calibrated⁶² for laser wavelengths. This instrument is not ideally suited for the determination of very small dn/dc values; we are satisfied that $dn/dc < 0.02$ mL/g at $\lambda_0 = 5145$ Å. The optical properties of PSLG prepared by transesterification of PBLG or another polypeptide could be considerably different, as transesterification is never 100% complete. Such materials are rightly considered copolymers. For the homopolymers presently under study, a reasonably good index match is assured. A relevant consideration is the ratio of the intensity scattered by PS to that scattered by PSLG. Neglecting form factor corrections, the intensity scattered by a polymer is

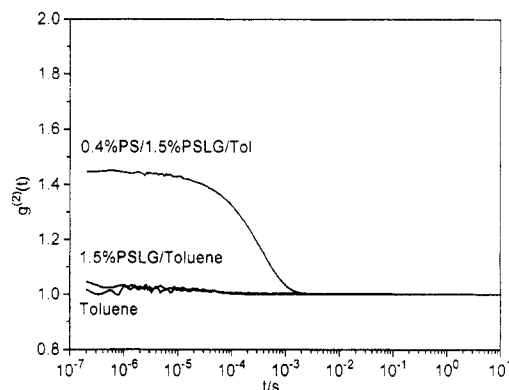


Figure 4. A 1.5% PSLG/toluene solution scatters scarcely more than pure toluene itself. Upon addition of 0.4% PS, coherent scattering is immediately apparent. The optical parameters and acquisition times were identical for all three samples.

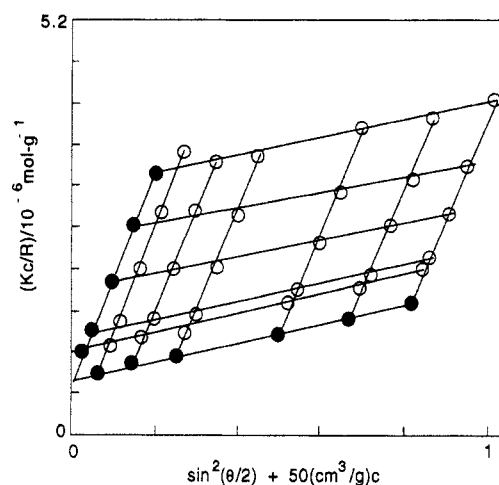


Figure 5. Zimm plot for PS in the complex solvent PSLG/toluene.

proportional to its concentration, mass, and $(dn/dc)^2$. Assuming that PSLG exists predominantly as pentamers, PS still outscatters it by a factor of about 200 at equal concentrations if dn/dc of PSLG/toluene is 0.02 mL/g and dn/dc of PS/toluene is 0.11 mL/g.⁶³ In dilute solutions of homopolymeric PSLG, it is difficult to measure any scattering in excess of the toluene. M , R_g , and A_2 changed insignificantly when the intensity of pure toluene was used to compute the excess scattered intensity, instead of the intensity scattered by PSLG/toluene complex solvent. Correlation functions of PSLG/toluene binary solutions exhibit very low coherence, even for spectrometer settings that yield high values of the coherence parameter f_{coh} for strongly scattering polymer/solvent systems, such as PS in toluene. This is shown in Figure 4, where the ALV-5000 correlator has been used to measure pure toluene, binary PSLG/toluene, and ternary PS/PSLG/toluene over a very wide range of delay times, under exactly identical conditions.

Static Light Scattering. Previous studies on ternary random-coil systems show that the addition of one polymer abruptly changes the apparent thermodynamic environment of the other, as judged from decreased apparent second virial coefficients.⁶⁴⁻⁶⁷ There is a disagreement on the magnitude of the effect of another polymer on R_g and the concentration at which the effect is observed.^{65,66}

A Zimm plot for PS in 0.2% PSLG/toluene is shown in Figure 5. The purpose of this plot is to display typical data in a familiar form; as already discussed, the analysis did not follow the linear Zimm prescription. The apparent molecular weight, radius of gyration, and second osmotic virial coefficient of PS were determined as functions of

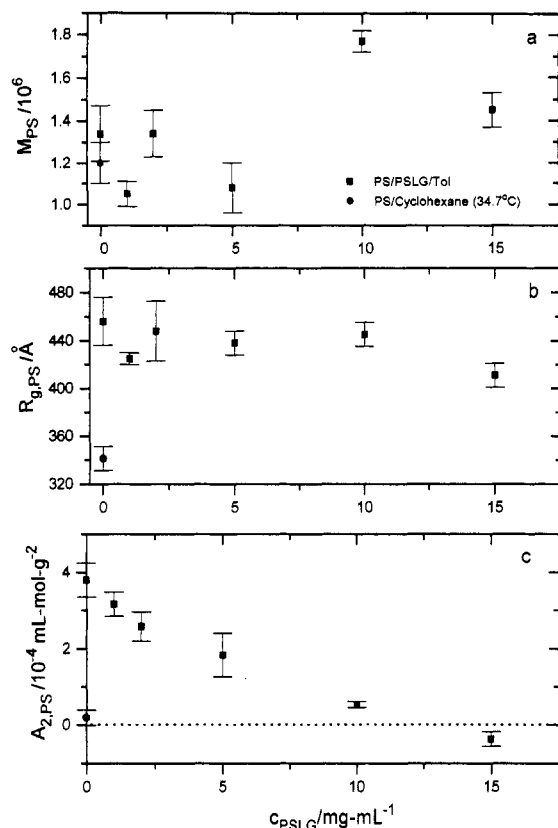


Figure 6. Static light scattering results. Squares: PS in toluene or PS/toluene complex solvent. Circles: PS under Θ conditions (cyclohexane, 34.7 °C).

c_{PSLG} . As shown in Figure 6a, the apparent molecular weight is generally in good agreement with the manufacturer's claim, except perhaps near $c_{\text{PSLG}} = 0.01$ g/mL. A possible cause of the random variations in M_{PS} is concentration error due to the small volumes of stock solutions that were mixed together in order to conserve PSLG for other experiments. Systematic molecular weight deviations associated with incomplete index matching have been observed and discussed elsewhere.^{19,20} Their absence here suggests adequate index matching of PSLG and toluene. Figure 6b shows that $R_{g,\text{PS}}$ does not change much with added PSLG. In contrast, $A_{2,\text{PS}}$ decreases strongly with c_{PSLG} and an apparent Θ condition is reached at about 1.4% PSLG; see Figure 6c. The same PS sample was measured under conventional binary solution Θ conditions (cyclohexane, $T = 34.7$ °C). The radius of gyration in binary solution, 340 Å, is in good agreement with literature values for this molecular weight⁵⁸ but about 30% smaller than in ternary PS/PSLG/toluene at the apparent Θ concentration. Thus, the reduction in virial coefficient with added PSLG is accomplished without the coil contraction found under typical binary solution Θ conditions. Kuhn and Cantow⁶⁶ applied the Stockmayer theory of scattering from multicomponent solutions⁶⁷ to explain decreases in apparent second virial coefficients for the visible component. Kent et al.¹⁹ extended the Stockmayer theory to terms of order c^3 . From equations such as (A.7) of ref 19 one can, in principle, determine various binary and ternary virial coefficients. This pursuit is hampered in the present case by uncertainty in the molecular weight of the aggregating PSLG matrix component.

Dynamic Light Scattering. Either by virtue of slight refractive index mismatch⁶⁸ or by virtue of cooperative modes for the case of a perfect match,⁴⁵⁻⁴⁸ two decay modes are expected in this system. An autocorrelation function at high scattering angle for the sample with highest PSLG concentration ($c_{\text{PSLG}} = 0.015$ g/mL; $c_{\text{PS}} = 0.004$ g/mL; c_{total}

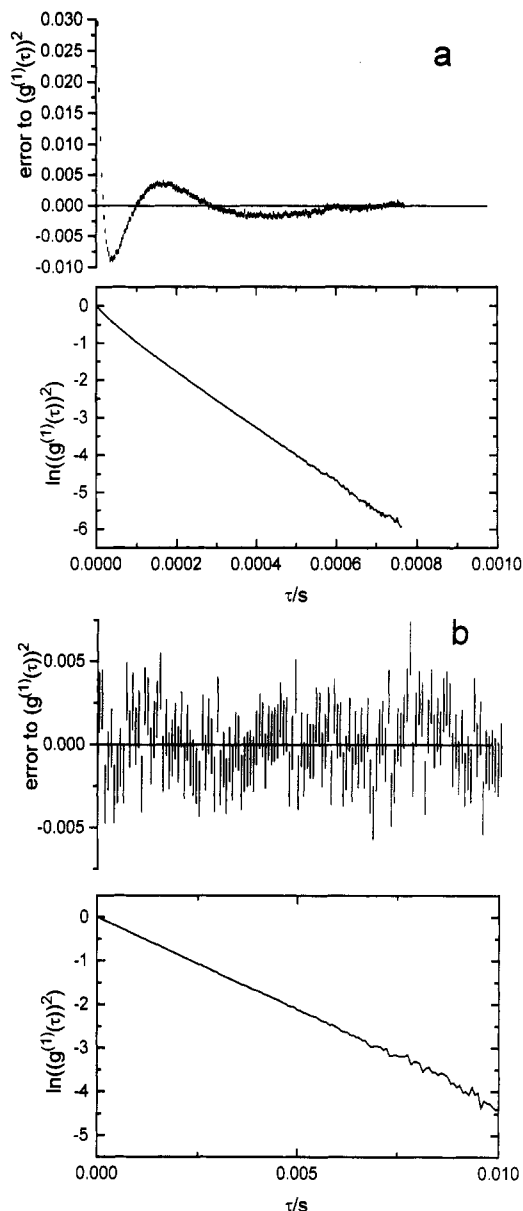


Figure 7. (a) Semilogarithmic plot of a normalized, second-order autocorrelation function, with associated residuals for 3CUMU fit; $\theta = 130^\circ$. (b) Same as a but $\theta = 30^\circ$. For both a and b the height of the bars in the residuals plots represents the uncertainty of measurement. In b almost all the bars touch the horizontal line of zero error; the data are fit to within their uncertainty. This is not the case for a where the correlation function is more nonexponential.

$= 0.019$; $x = 0.21$) is shown in Figure 7a. This correlation function, which exhibited more non-single-exponential behavior than any other, is bimodal, but the faster component comprises only about 12% of the total scattering amplitude, as judged by double-exponential analysis. The residuals plot shows that the 3CUMU analysis "misses" in the early channels by up to 3% of $g^{(2)}(\tau) - 1$ but does a better job at fitting the slower components. Thus, with the channel times set as they were, the 3CUMU fit effectively concentrates on the slower mode. The $\mu_2/\bar{\Gamma}^2$ nonexponentiality parameter was 0.3. CONTIN or other Laplace inversion analysis is generally warranted when $\mu_2/\bar{\Gamma}^2$ exceeds about 0.25; therefore, at the highest angles it would be possible to resolve the two decay modes with poor-fair precision. The decay rate distributions were effectively unimodal for solutions containing less PSLG and also for high-PSLG solutions at lower angle. Figure 7b shows a correlation function for the same sample as in Figure 7a but this time measured at $\theta = 30^\circ$. In this case, $\mu_2/\bar{\Gamma}^2$ is approximately 0.15 and deviations from linearity

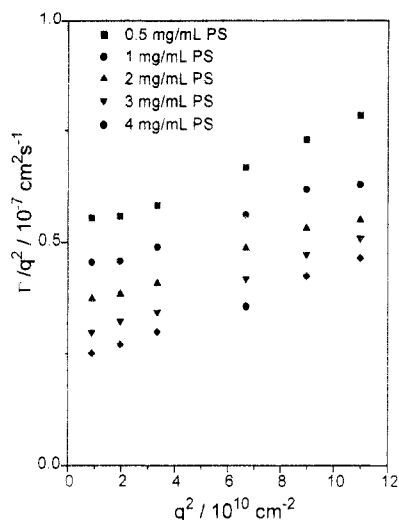


Figure 8. Dependence of the apparent first cumulant upon the scattering vector. The PSLG content was 15 mg/mL; concentrations of PS are as indicated. Mutual diffusion coefficients of the PS component were taken from the intercepts.

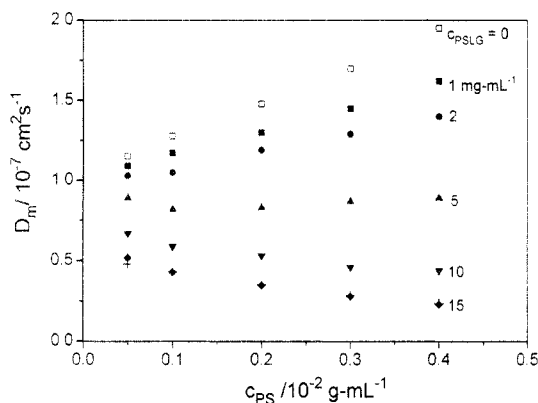


Figure 9. Mutual diffusion coefficient of the PS component vs concentration of the PS component, for various PSLG contents. Open square: pure toluene. Full symbols from top to bottom: PSLG = 1, 2, 5, 10, and 15 mg/mL. The bottom data set actually shows two overlapping points (plus and diamond) at each value of c_{PS} . The pluses represent the slower mode of a two-exponential analysis. The diamonds (and all other data on the graph) come from cumulants analysis.

are far less obvious. Thus, although a weak rapid decay mode is present in these systems, the 3CUMU analysis is adequate for identification of the main decay mode.

The apparent diffusion coefficient $\bar{\Gamma}/q^2$ was a function of q^2 in all cases, as shown in Figure 8. Linear least-squares extrapolation of $\bar{\Gamma}/q^2$ to zero angle yields $D_m(c_{PS}, c_{PSLG})$. Given the admonitions of refs 49 and 50, we are reluctant to refer to the diffusion coefficient associated with the measured main decay mode as "interdiffusion". Instead, we simply call it $D_m = D_m(c_{PS}, c_{PSLG})$ as discussed already. When extrapolated to $x = 0$, $D_m \rightarrow D_o = D_o(c_{PSLG})$. It is expected that D_o resembles closely the polystyrene self-diffusion coefficient D_s . As c_{PSLG} increases, both the intercept and the slope of the $D(c_{PS}, c_{PSLG})$ vs c_{PS} line change, as shown in Figure 9.

Intercepts of Figure 9 provide $D_o(c_{PSLG})$. The result, Figure 10, can be compared with the stretched-exponential expression, $D \sim \exp(-\alpha c_{PSLG}^\nu)$. The accurate fitting of parameters to a stretched-exponential form is notoriously difficult, especially in the present case where the number of data points is small. If it is assumed that $\nu \sim 1$, then the value $\alpha = 0.41 \pm 0.03$ mL/g is obtained from a linear fit of $\log D$ vs c . A nonlinear least-squares fit (using MicroCal Origin, Version 2.8) yields $\nu = 1.32 \pm 0.14$ and $\alpha = 0.39 \pm 0.02$ (mL/g) $^{1/\nu}$. The analysis was

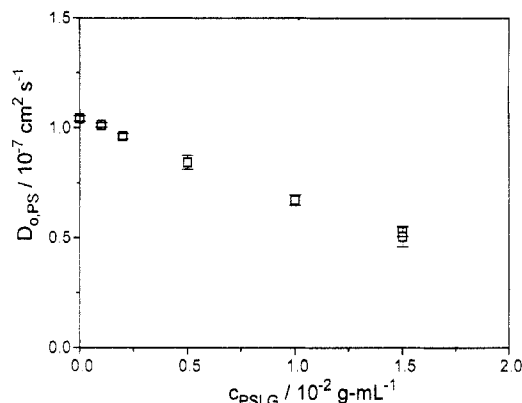


Figure 10. Decrease in $D_{o,PS}$ with an added rodlike component in the PSLG/toluene complex solvent.

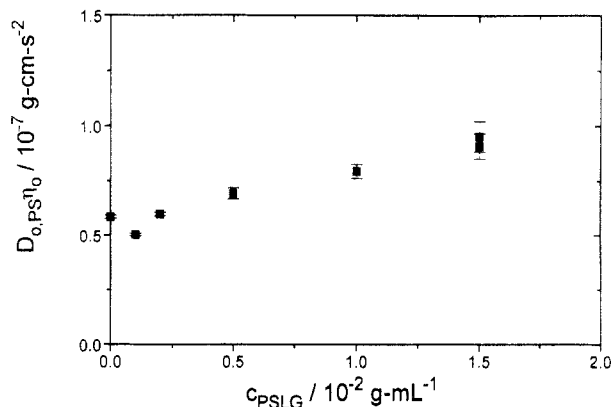


Figure 11. Viscosity of the complex solvent which increases more rapidly with an added rodlike component than diffusion of a coil component decreases.

repeated by replotting c^ν and visually observing the onset of nonlinearity.³³ This yields $\nu = 1.35 \pm 0.15$ and $\alpha = 0.58 \pm 0.04$ (mL/g) $^{1/\nu}$. In summary, $\nu \approx 1.3$ and $\alpha \approx 0.5$. Experimental values for ν are typically smaller in most other systems, while a variety of theories predict $\nu = 0.5$ – 1.0 .³ The large value reported here probably reflects the end-to-end aggregation of PSLG.

The translational diffusion of polymers in a dilute binary solution of small solvent molecules defines a hydrodynamic radius, R_h , through the Stokes–Einstein (SE) relation:

$$\eta_o D_o = k_B T / 6\pi R_h$$

where η_o is the solvent viscosity and $k_B T$ is the molecular thermal energy of the diffuser. To extend the notation to ternary systems, we let $\eta_o = \eta_o(c_{PSLG})$ —similar to the definition of D_o in that probe concentration dependence has been extrapolated away. We also stipulate that η_o represents a zero-shear rate viscosity: η_o is the viscosity of the complex solvent at zero-shear rate. There is no guarantee that a SE regime exists in ternary systems. If a complex solvent contains components comparable in size to the probe or if there exists a correlation length ξ comparable in size to R_g , then the probe may not be constrained to move only as fast as thermal energy and the macroscopic solution viscosity allow. Rather, it may slip through the constraints and move faster. If a SE regime exists, the product $\eta_o D_o$ would be constant; Figure 11 shows that it is not. The reduction in D_o for a PS chain with increasing c_{PSLG} is clearly less than the corresponding viscosity increase of the PSLG solution. In principle, one should first take into consideration probe chain contraction; however, Figure 6b shows that this effect is mild in the present case.

Large failures of the SE relation are not uncommon for random-coil diffusers^{8,9,21} that may reptate past relatively

stationary topological constraints. Somewhat more surprising are large failures of the SE relationship that have even been reported for solid spherical probes.^{3,69} The hypothesis that reptative motion or alternative mechanisms enable random coils to diffuse more rapidly through entangled polymer solutions than a simple sphere of similar hydrodynamic radius is controversial. Here we can only consider the case of the linear coil probe. Martin developed scaling relationships to describe the crossover from SE diffusion to reptation for random-coil probes immersed in a random-coil matrix.^{8,9} In the reptation limit, the product $\eta_0 D_0$ was predicted (and experimentally found) to scale with concentration as c^γ where $\gamma \sim 2$. (The theoretical value depends slightly on assumptions involving the screening of thermodynamic interactions.) The scaling argument is easily extended to the case of a random-coil probe immersed in a (nonaggregating) matrix of rods; see the Appendix. The result in the reptation limit is a stronger deviation from SE behavior: $\gamma = 11/4$. The present data are not well suited to test this relationship, as the entanglement concentration for the rods is never greatly exceeded and the rods aggregate. A log-log plot of the data in Figure 11 gives a very weak slope of only about 0.2.

Slopes of Figure 9 represent the dependence of D_m on c_{PS} for given values of c_{PSLG} . The parameter k_d is defined through $D_m = D_0(c_{PSLG})(1 + k_d c_{PS})$. This definition adheres to eq 20 rather than eq 12 of ref 20, where D_0 is defined as the infinite dilution value of the probe diffusion coefficient in a binary solution. The usual expression⁷⁰ describing how D_m depends on c in binary solutions is $k_d \approx 2A_2M - k_f - \nu$ where k_f is the linear term in a concentration expansion for the mutual friction factor, f_m , and ν is the partial specific volume of the probe polymer. In deriving this expression,⁷⁰ the quotient of competing thermodynamic and friction terms is expanded, retaining only the linear terms in k_f and concentration. In most binary solutions under good solvent conditions, excluded-volume interactions between the polymers increase in importance more rapidly than the mutual friction factor, so D_m increases with c . That is, random fluctuations to produce locally high polymer concentrations demand rapid relaxation.

Following the initial observations of Chang et al.,¹⁵ Kent et al.^{19,20} developed a theory that extends the concepts of the previous paragraph to ternary solutions. Heuristically, a probe polymer has much less cause to diffuse away from locally high concentrations if, when it does, it remains surrounded by matrix. The same reasoning accounts for the reduction in $A_{2,PS}$ even though $R_{g,PS}$ remains relatively constant; two probe chains that would strongly avoid mutual overlap to maximize their configurational entropy in a binary solution have no cause to dodge each other if the available space is occupied by other polymers anyway. This argument is entropic and does not rest on unfavorable enthalpic interactions between the probe and matrix. Any such interaction hastens the decrease in k_d and favors negative k_d . Kent et al. observed a rapid decrease in k_d to a minimum at a negative value, followed by a return to a less negative value as the mutual friction term became more important, for the system PS/PMMA/ethyl benzoate, in which PS and PMMA have a slightly unfavorable interaction (PMMA = poly(methyl methacrylate)). They were able to account for this behavior by deriving an expression for k_d in ternary solutions. Equation 19 of ref 20 again pits thermodynamic driving terms against friction terms. But the presence of the matrix polymer alters the relative importance of the two effects, so the quotient is not expanded, linear approximations are avoided, and nonmonotonic behavior can be described. In the present case, k_d decreases rapidly (Figure 12) but it does not pass

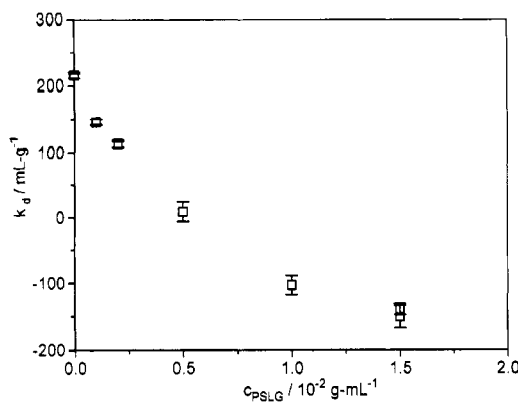


Figure 12. k_d changes from positive to negative as the rodlike character of the complex solvent increases.

through a minimum in the measured range, although the curvature is positive. Perhaps this suggests that the interaction between PS and PSLG is more unfavorable than that between PS and PMMA, so that the thermodynamic term remains more prominent in the available concentration range.

Conclusion

Addition of PSLG with its waxy side chains to a PS/toluene solution has two consequences: introduction of some aliphatic character, an enthalpic effect; plus, occupation of considerable amounts of highly linearly correlated space that the PS coil must avoid, an entropic consideration. To gauge the relative importance of these factors, a 5% dodecane/95% toluene mixture was prepared volumetrically. This mixed solvent has considerably more aliphatic character than the highest PSLG solution studied. Yet polystyrene dissolved in it showed no sign of being in a poor or θ solvent: $A_{2,app}$ was strongly positive and k_d was identical to that in binary PS solutions in pure toluene. Although PS and PSLG probably do have a positive enthalpy of mixing, the effects observed here trace predominantly to the occupation by the rods of linearly connected sites that restrict the possible random-coil conformations.

The contraction of coils under the influence of other coils has been considered theoretically⁷¹ and experimentally.^{20,72,73} Size is usually observed to vary according to $R_g \sim c^{-1/8}$. The contraction of a coil surrounded by rods may be less, because one way for the coil to avoid the rods is to favor conformations that enable it to run nominally straight over distances comparable to the correlation length of the rods. A scaling argument (see Appendix) suggests $R_{g,coil} \sim c_{rod}^{-1/12}$. The present data, showing virtually no dependence of coil radius on rod concentration, offer no evidence to support this relationship, probably because the concentration range of the rods is too limited. Similarly, higher matrix concentrations will be required to determine whether the Stokes-Einstein failures reported here can be explained as a crossover to reptation. The search continues for a system in which the rodlike matrix concentration can approach the internal segment density of the random coils, without risk of phase separation. Covalently cross-linked networks of rods should not be overlooked during this search.

Acknowledgment. This work was supported by the National Science Foundation. Helpful conversations with Dr. D. K. Carpenter of Louisiana State University are gratefully acknowledged.

Appendix. Scaling Relationships for Random Coils Immersed in Semidilute Rods.

Coil Contraction. In the standard argument⁷¹ for a binary semidilute solution of a random coil, the radius of

gyration is written in the Gaussian limit:

$$R_g^2 \sim (N/N_b)\xi^2 \quad (\text{A1})$$

where N is the number of monomers and N_b the number of monomers in a "blob" of dimension ξ , the correlation length, beyond which excluded-volume interactions are screened. Within the correlation length, the standard Flory result is assumed, yielding

$$\xi \sim N_b^{3/5} \quad (\text{A2})$$

Inserting A2 into A1 yields $R_g^2 \sim \xi^{1/3}$. As $\xi \sim c^{-3/4}$ for random coils, the result is $R_g \sim c^{-1/8}$. For a random coil immersed in a filamentous matrix, eqs A1 and A2 should still be valid, but $\xi \sim c^{-1/2}$ for rods^{62,74,75} leads to a weaker concentration dependence for the coil radius, $R_{g,\text{coil}} \sim c_{\text{rod}}^{-1/12}$.

Stokes-Einstein to Reptation Crossover. Following Martin,^{8,9} we write the ratio of reptative (τ) to Stokes-Einstein (SE) diffusion as:

$$D_r/D_{SE} = (R^2/\tau_r(N))/(kT/6\pi\eta R) \sim R^3\eta/\tau_r(N)$$

Here, $\tau_r(N) \sim N^3$ is the reptation time for the coil, and η is the solution viscosity, determined primarily by the rodlike matrix. According to eq A1 and A2, $D_r/D_{SE} = \xi^{1/2}N^{3/2}\eta_{\text{rods}}$. As $\xi \sim c^{-1/2}$ and $\eta \sim c^3$ for rods^{62,74,75,76} the result is

$$D_r/D_{SE} = c^{11/4}/N^{3/2}$$

References and Notes

- Turner, D. N.; Hallett, F. R. *Biochem. Biophys. Acta* **1976**, *451*, 305.
- Langevin, D.; Rondelez, F. *Polymer* **1978**, *19*, 875.
- Phillies, G. D. J. *J. Phys. Chem.* **1989**, *93*, 5029.
- Brown, W.; Rymden, R. *Macromolecules* **1988**, *21*, 840.
- Onyenezazu, C. N.; Gold, D.; Roman, M.; Miller, W. G. *Macromolecules* **1993**, *26*, 3833.
- Lodge, T. P. *Macromolecules* **1983**, *16*, 1393.
- Cotts, D. B. *J. Polym. Sci., Polym. Phys. Ed.* **1983**, *21*, 1381.
- Martin, J. E. *Macromolecules* **1984**, *17*, 1279.
- Martin, J. E. *Macromolecules* **1986**, *19*, 922.
- Numasawa, N.; Hamada, T.; Nose, T. *J. Polym. Sci. Polym. Phys. Ed.* **1985**, *23*, 1.
- Numasawa, N.; Hamada, T.; Nose, T. *J. Polym. Sci., Polym. Phys. Ed.* **1986**, *24*, 19.
- Chu, B.; Wu, D.-Q. *Macromolecules* **1987**, *20*, 1606.
- Borsali, R.; Duval, M.; Benoit, H.; Benmouna, M. *Macromolecules* **1987**, *20*, 1112.
- Giebel, L.; Borsali, R.; Fischer, E. W.; Meier, G. *Macromolecules* **1990**, *23*, 4054.
- Chang, T.; Han, C. C.; Wheeler, L. M.; Lodge, T. P. *Macromolecules* **1988**, *21*, 1870.
- Phillies, C. D. J.; Clomenil, D. *Macromolecules* **1993**, *26*, 167.
- Konak, C.; Tuzar, Z.; Jakes, J. *Polymer* **1990**, *31*, 1866.
- Aven, M. R.; Cohen, C. *Macromolecules* **1990**, *23*, 476.
- Kent, M. S.; Tirrell, M.; Lodge, T. P. *Polymer* **1991**, *32*, 314.
- Kent, M. S.; Tirrell, M.; Lodge, T. P. *Macromolecules* **1992**, *25*, 5383.
- Lodge, T. P.; Wheeler, L. M. *Macromolecules* **1986**, *19*, 2983.
- Lodge, T. P.; Markland, P.; Wheeler, L. M. *Macromolecules* **1989**, *22*, 3409.
- Lodge, T. P.; Rotstein, N. A.; Prager, S. *Adv. Chem. Phys.* **1990**, *LXXIX*, 1.
- Nishio, I.; Reina, J. C.; Bansil, R. *Phys. Rev. Lett.* **1987**, *59*, 684.
- Newman, J.; Mroczka, N.; Schick, K. L. *Biopolymers* **1989**, *28*, 655.
- Joosten, J. G. H.; Gelade, E. T. F.; Pusey, P. N. *Phys. Rev. A* **1990**, *42* (4), 2161.
- Bishop, M. T.; Langley, K. H.; Karasz, F. E. *Macromolecules* **1989**, *22*, 1220.
- Guo, Y.; Langley, K. H.; Karasz, F. E. *Macromolecules* **1992**, *25*, 4902.
- Brown, W.; Rymden, R. *Macromolecules* **1986**, *19*, 2942.
- Yang, T.; Jamieson, A. M. *J. Colloid Interface Sci.* **1988**, *126*, 220.
- Russo, P. S.; Stephens, L. K.; Cao, T.; Mustafa, M. *J. Colloid Interface Sci.* **1988**, *122*, 120.
- Mustafa, M.; Russo, P. S. *J. Colloid Interface Sci.* **1989**, *129*, 240.
- Tracy, M.; Pecora, R. *Macromolecules* **1992**, *25*, 337.
- Tracy, M. A.; Garcia, J. L.; Pecora, R. *Macromolecules*, in press.
- Flory, P. J. *Macromolecules* **1978**, *11*, 1138.
- The Materials Science and Engineering of Rigid Rod Polymers*; Materials Research Society: Pittsburgh, PA, 1989.
- Poche, D. S. Ph.D. Thesis, Synthesis and Characterization of Linear and Star-branched poly(γ -stearyl- α -L-glutamate). Louisiana State University, Baton Rouge, LA, 1990.
- Daly, W. H.; Poche, D. S. *Polym. Prepr. (Am. Chem. Soc., Div. Polym. Chem.)* **1989**, *30* (1), 107.
- Poche, D. S.; Daly, W. H.; Russo, P. S. *Polym. Prepr. (Am. Chem. Soc., Div. Polym. Chem.)* **1990**, *31* (2), 418.
- Daly, W. H.; Poche, D. S. *Tetrahedron Lett.* **1988**, *29* (46), 5859.
- Phillies, G. D. J. *J. Chem. Phys.* **1974**, *60*, 976.
- Phillies, G. D. J. *J. Chem. Phys.* **1974**, *60*, 983.
- Phillies, G. D. J. *Biopolymers* **1975**, *14*, 499.
- Pusey, P. N.; Fijnaut, H. M.; Vrij, A. *J. Chem. Phys.* **1982**, *77*, 4270.
- Akcasu, A. Z.; Benmouna, M.; Benoit, H. *Polymer* **1986**, *27*, 1935.
- Benmouna, M.; Benoit, H.; Duval, M.; Akcasu, A. Z. *Macromolecules* **1987**, *20*, 1107.
- Benmouna, M.; Benoit, H.; Borsali, R.; Duval, M. *Macromolecules* **1987**, *20*, 2620.
- Foley, G.; Cohen, C. *Macromolecules* **1987**, *20*, 1891.
- Akcasu, A. Z.; Tombakoglu, M. *Macromolecules* **1990**, *23*, 607.
- Akcasu, A. Z.; Nagele, G.; Klein, R. *Macromolecules* **1991**, *24*, 4408.
- Russo, P. S.; Saunders, M. J.; DeLong, L. M.; Kuehl, S. K.; Langley, K. H.; Detenbeck, R. W. *Anal. Chim. Acta* **1986**, *189*, 69.
- Koppel, D. E. *J. Chem. Phys.* **1972**, *57*, 4814.
- Haller, H. R.; Destor, C.; Cannell, D. S. *Rev. Sci. Instrum.* **1983**, *54*, 973.
- Kaye, W.; McDaniel, J. B. *Appl. Opt.* **1974**, *13*, 1934.
- Leite, R. C. C.; Moore, R. S.; Porto, S. P. S.; Ripper, J. E. *Phys. Rev. Lett.* **1965**, *14*, 7.
- Wiltzius, P.; Haller, H. R.; Cannell, D. S.; Schaefer, D. W. *Phys. Rev. Lett.* **1983**, *51* (13), 1183.
- Zimm, B. H. *J. Chem. Phys.* **1948**, *16*, 1093.
- Berry, G. C. *J. Chem. Phys.* **1966**, *44* (12), 4550.
- Chakrabarti, S.; Miller, W. G. *Biopolymers* **1984**, *23*, 719.
- Schmidt, P. W. In *The Fractal Approach to Heterogeneous Chemistry: Surfaces, Colloids, Polymers*; Avnir, D., Ed.; Wiley: New York, 1989; Section 2.2, pp 55-66.
- Porod, G. In *Small Angle X-ray Scattering*; Glatter, O.; Kratky, O., Eds.; Academic Press: New York, 1982; Chapter 2.
- DeLong, L. M.; Russo, P. S. *Macromolecules* **1991**, *24*, 6139.
- Huglin, M. B. In *Light Scattering from Polymer Solutions*; Huglin, M. B., Ed.; Academic Press: New York, 1972; Chapter 6.
- Stockmayer, W. H.; Stanley, H. E. *J. Chem. Phys.* **1950**, *18*, 153.
- Hyde, A. J.; Tanner, A. G. *J. Colloid Interface Sci.* **1968**, *28*, 179.
- Kuhn, R.; Cantow, H. J. *Makromol. Chem.* **1969**, *122*, 65.
- Stockmayer, W. H. *J. Chem. Phys.* **1950**, *18*, 58.
- Lodge, T. P.; Wheeler, L. M.; Hanley, B.; Tirrell, M. *Polym. Bull. (Berlin)* **1986**, *15*, 35.
- Phillies, G. D. J.; Brown, W.; Zhou, P. *Macromolecules* **1992**, *25*, 4948.
- Yamakawa, H. *Modern Theory of Polymer Solutions*; Harper and Row: New York, 1971; Section 30.
- de Gennes, P.-G. *Scaling Concepts in Polymer Physics*; Cornell University Press: Ithaca, NY, 1979; Section III.2.5.
- Daoud, M.; Cotton, J. P.; Farnoux, B.; Jannink, G.; Sarma, G.; Benoit, H.; Duplessix, R.; Picot, C.; de Gennes, P.-G. *Macromolecules* **1975**, *8*, 804.
- King, J. S.; Boyer, W.; Wignall, G. D.; Ullman, R. *Macromolecules* **1985**, *18*, 709.
- de Gennes, P.-G.; Pincus, P.; Velasco, R. M.; Brochard, F. *J. Phys. (Paris)* **1976**, *37*, 1461.
- Shimada, T.; Doi, M.; Okano, K. *J. Chem. Phys.* **1988**, *88*, 2815.
- Doi, M.; Edward, S. F. *The Theory of Polymer Dynamics*; Oxford Science: Oxford, U.K., 1989; Chapter 9.